Frequency domain analysis of membrane capacitance of cultured cells (HeLa and myeloma) using the micropipette technique

K. Asami*, Y. Takahashi‡, and S. Takashima§

*Institute for Chemical Research, Kyoto University, Uji, Kyoto, Japan; ‡Olympus Optical Company, Hachioji, Tokyo, Japan; and §Department of Bioengineering, University of Pennsylvania, Philadelphia, Pennsylvania 19104-6392 USA

ABSTRACT The membrane capacitance and conductance of cultured cells (HeLa and mouse myeloma) are investigated using the micropipette method. Mean values of the membrane capacities were found to be 1.9 $\mu F/cm^2$ for HeLa cells and 1.0 $\mu F/cm^2$ for myeloma cells. These values are in agreement with those obtained using the suspension method. Whereas the suspension method is unable to provide the information on membrane conductance, the micropipette method is able to measure even an extremely small membrane conductance if leakage current is negligibly small. The membrane conductances were found, using this technique, to be ~90–100 $\mu S/cm^2$ for both HeLa and myeloma cells. One of the purposes of this study is to establish the frequency profile of membrane capacitance. It was found, however, that membrane capacitances of these cells are independent of frequency between 1 Hz and 1 KHz within the resolution of this technique.

INTRODUCTION

A variety of techniques have been employed for the frequency domain analysis of membrane admittance of the biological cells (1). The use of an internal electrode and various types of gap methods enables the transmembrane admittance to be measured directly and accurately without a cumbersome mathematical manipulation. These techniques have been used for some excitable cells such as the giant axon of squid (2–4) and frog skeletal muscle fibers (5–7), where the size and geometry are suitable for these electrode arrangements. However, many biological cells such as erythrocyte and lymphocyte are very small and their geometries are unsuitable for the use of an internal electrode or the gap method. To circumvent the technical difficulties of admittance measurement with these cells, we developed a micropipette technique which enables us to perform the frequency domain analysis of the membrane admittance of small spherical cells between 1 Hz and 1 KHz. The micropipette used for this technique is very similar to those used for the patch clamp method by Hamill et al. (8, 9). In a previous paper, we reported the results of the capacitance and conductance measurements with human erythrocyte using micropipettes (10).

Human erythrocyte is, however, not necessarily the most suitable preparation for this technique because of a very small total membrane capacitance, i.e., ~1 pF and is close to the limit of the resolution of the manually operated micropipette method. Our strategy for improvements is twofold; one is to increase the resolution of the measuring system and to reduce the data acquisition time by the use of an on-line computer. The reduction of data acquisition time eliminates the error resulting from the deterioration of specimens during measurements. In addition to this improvement, cultured cells having a larger total capacitance were used. The results of admittance measurements with HeLa and mouse myeloma cells are discussed in this paper. Similar measurements with cultured excitable cells such as neuroblastoma and myoblastoma L6 cells are underway at present and the results will be published elsewhere. One of the purposes of these measurements is to study the frequency profile of membrane capacitance and conductance which is often useful for the analysis of the mechanism of electrical polarization of the polymer solutions and/or biological membranes. Membrane proteins, channel proteins in particular, are believed to have a large dipole moment (11, 12). The orientation of these molecules in a viscous medium gives rise to a frequency dependent capacitance. If membrane structure is rigid and protein molecules have no freedom of orientation, then, membrane capacitance will be similar to that of pure lipid bilayers without noticeable frequency dependence.

Address correspondence to Dr. Takashima.

MATERIAL AND METHODS

Preparation of cells

HeLa and mouse myeloma (P3X63Ag8) cells were purchased from American Type Culture Collection (Rockville, MD) and grown in plastic tissue culture dishes or bottles in Dulbeco's modified Eagle medium supplemented with 10% fetal bovine serum at 37°C.

0006-3495/90/07/143/06 $2.00

Micropipette method

Micropipettes were made of borosilicate glass capillaries after the procedure of Hamill et al. (8) using a vertical microelectrode puller. Micropipettes were heat polished immediately before use and were filed with a solution: 140 mM KCl, 2 mM $MgCl_2$, 11 mM EGTA-KOH, 1 mM $CaCl_2$, 10 mM HEPES-KOH, and pH 7.2. This is a mimetic salt solution of the mammalian cytoplasm, and is suitable for the whole cell recording. The electrode tip resistance with this internal solution ranged between 10–20 Mohms.

Before admittance measurements, the culture medium was replaced with Dulbecco's phosphate buffer saline (PBS). HeLa cells were pretreated with a trypsin solution (0.25% trypsin in PBS without $CaCl_2$ and $MgCl_2$), to transform them into spherical cells. The trypsin pretreatment was not necessary for myeloma cells.

The admittance measurements were carried out in the three configurations described by Hamill: cell-attached, whole cell, and outside-out modes. At first, a tight seal (giga seal) was established between cell membrane and the pipette tip by applying a weak suction of ~20–30 cm H_2O. Once a resistance of 10 Gohm or more is attained, the seal is mechanically as well as electrically stable, even after the negative pressure is released. To attain the whole cell configuration, a stronger suction of ~100 cm H_2O is applied until a sudden increase in V_o is noted, an indication of the rupture of the membrane patch inside the pipette tip. Finally, an outside-out patch was obtained by withdrawing the pipette tip from the cell surface.

Electrical apparatus

We improved the impedance measuring system which was described in a previous paper (10). Fig. 1 shows a block diagram of the system. Sinusoidal waves were generated by a voltage-controlled oscillator (Lockin Amplifier 124; Princeton Applied Research, Princeton, NJ). The frequency was controlled by the voltage output of a computer (IBM AT) via a digital-to-analog converter (Lab Master 12 bits resolution). Sinusoidal waves with a voltage V_i (20–40 mV p-p) was applied between two Ag-AgCl electrodes, the one in the micropipette and the other in a salt bridge (see Fig. 1). The current passed through a cell membrane was measured with a current amplifier (model 427 Current Amplifier; Keithley Instruments, Inc., Cleveland, OH). The output voltage V_o and input voltge V_i were sampled simultaneously by an A/D converter (Lab Master, 30 KHz 12 bits resolution; Scientific Solutions, Inc., Solon, OH). The total data acquisition time was <1 min when 31 frequency points were scanned between 1 Hz and 1 KHz.

Collected data points were fitted to sinusoidal waveforms by the least square minimization method to determine the amplitude (A) and phase angle (θ) of output voltage (V_o) relative to the input voltage (V_i). Based on the electrical circuit illustrated in Fig. 2, we can relate the parameters A (or the voltage ratio V_o/V_i) and θ to the sample (Y_x) and feedback admittances (Y_f) as

$$V_o/V_i = A(\cos\theta + j\sin\theta) = Y_x/Y_f. \quad (1)$$

Because admittances are given by the parallel combination of capacitance (C) and conductance (G), Y_x and Y_f are expressed as

$$Y_x = G_x + j\omega C_x \quad (2)$$

$$Y_f = G_f + j\omega C_f, \quad (3)$$

where $j = \sqrt{-1}$, $\omega = 2\pi f$, and f is frequency. Substituting Eqs. 2 and 3 in Eq. 1, we obtain the following equations.

$$C_x = A(C_f \cos\theta + G_f \sin\theta/\omega) \quad (4)$$

$$G_x = A(G_f \cos\theta - C_f\omega \sin\theta). \quad (5)$$

Fig. 3 shows a test run of this system with three dummy loads where (1) and (2) refer to cell-attached (see Fig. 7*c*) and whole-cell (see Fig. 5) configurations. (3) is an equivalent G-C parallel circuit of the model (2). The values of the components used in the dummy loads were chosen to simulate the admittances of HeLa and myeloma cells. The actual values of capacitors were measured using a Wayne Kerr admittance bridge B-221 and the values of precision resistors were provided by the manufacturer (Eltec Instruments, Daytona Beach, FL). The frequency dependence of the capacitance and conductance of curve 2 is due to the presence of a series resistance R_s. Curve 2 reduces to curve 4 after the correction for R_s using Eqs. 7 and 8 and subtracting the capacitances of curve 1 at each frequency. Curve 4 is virtually identical with curve 3, i.e., capacitance of the circuit (3). Thus, the results are consistent and are in agreement with the prediction. Based on these results, we can conclude that the resolution of this system, combined with the use of micropipettes, is sufficiently high for the admittance measurements of biological cells with proper averaging of the data.

Cell suspension method

To validate the results obtained by the micropipette method with the conventional "suspension technique," we performed concomitant measurements of the admittances using the suspension of both HeLa and myeloma cells in PBS. An impedance analyzer (model 4192A; Hewlett-Packard Co., Palo Alto, CA) operated by a microcomputer (model 216, Hewlett-Packard) were used as described in a previous paper (13). The membrane capacitance (C_m) of the cells was calculated from the

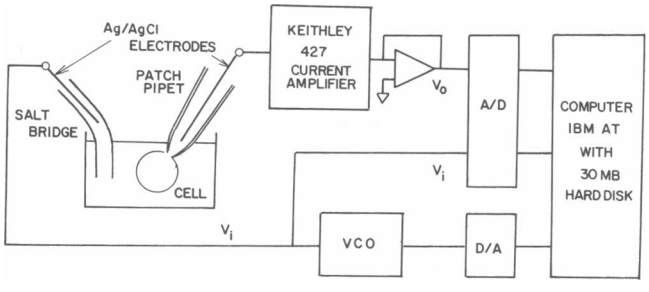

FIGURE 1 A schematic diagram of the experimental apparatus. VCO, a voltage controlled signal generator; V_i, input voltage; V_o, output voltage.

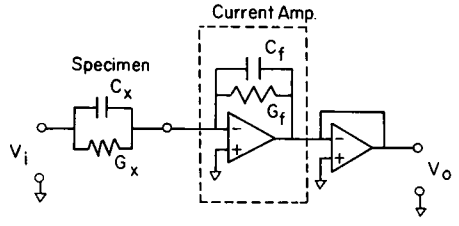

FIGURE 2 An equivalent circuit used for the calculation of sample admittance. C_x and G_x are the capacitance and conductance of sample. G_f is a feedback conductance and C_f(0.2 pF) is the parasitic capacitance of G_f.

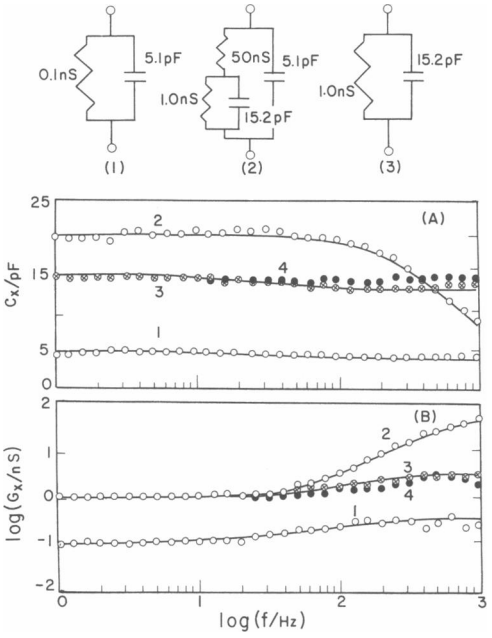

FIGURE 3 Test run of the admittance measurement system with three dummy loads. (*A*) Curve 1 represents the capacitive component of circuit (1), i.e., the cell attached configuration (see Appendix B). Curves 2 and 3 represent the capacitive components of (2) and (3), i.e., the whole cell configuration and its equivalent *G-C* parallel circuit. Curve 4 is obtained after correction for the series resistance R_s and subtracting the capacitances of curve 1 at each frequency. (*B*) Curves 1, 2, and 3 represent the conductances of the circuits (1), (2) and (3). Curve 4 is obtained after correction of curve 2 for series resistance.

following approximate equation derived from the Hanai-Asami-Koizumi (H-A-K) mixture equation (13–15). The derivation is shown in Appendix A.

$$C_m = \frac{2}{3}\frac{\epsilon_v}{R}\frac{\epsilon_l}{1 - k_l/k_a}, \tag{6}$$

where R is cell radius, ϵ_v is the permittivity of free space, k_a is the conductivity of suspending medium, and ϵ_l and k_l are the limiting relative permittivity and conductivity of the suspension at low frequencies.

RESULTS AND DISCUSSION

Micropipette method

Fig. 4 illustrates the results of the measurements using HeLa cells in the cell-attached configuration (1) followed by the whole-cell (2) and the outside-out (3) recording configurations. It should be noted that the results obtained with the cell-attached configuration is almost identical with that of the outside-out configuration. After the initial measurements with the cell-attached configuration, the whole-cell mode is formed by applying strong

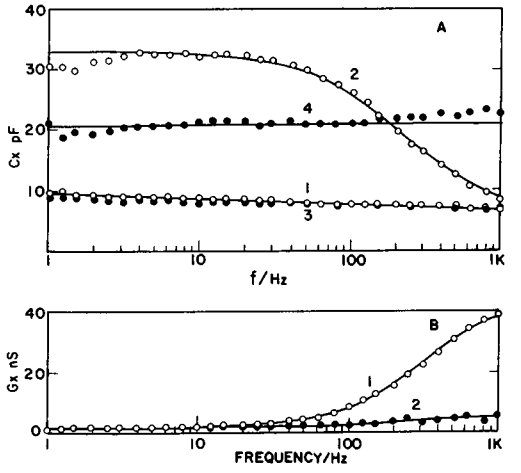

FIGURE 4 (*A*) Capacitances measured with HeLa cells in the cell-attached (*curve 1*), whole-cell (*curve 2*), and outside-out (*curve 3*) configurations. Curve 4 was obtained after the correction for the electrode or shunt capacitance and series conductance G_s using Eqs. 7 and 8. (*B*) Conductances measured with HeLa in the whole cell configuration before (*curve 1*) and after (*curve 2*) G_s correction.

suctions. The formation of the whole-cell configuration is detected by a sudden increase in V_0 indicating an increase in membrane capacitance and conductance due to the rupture of membrane patch within the pipette tip. As shown by curve 2 in Fig. 4, measured capacitance and conductance are several times larger than those of the cell-attached configuration. The decrease in measured capacitance at high frequencies does not reflect the real membrane electrical properties but is due to the artifacts arising from the series resistance owing to the large impedance of the micropipette tip. The detail of the corrections for series resistance and electrode capacitance is discussed below.

The whole-cell configuration may be represented by an equivalent circuit shown by the diagram (*a*) and in Fig. 5 in which membrane elements C_m and G_m along with a leakage conductance (G_l) is connected in series to the electrode conductance (G_s) as well as parallel to an electrode capacitance. The diagram (*b*) shows the equivalent parallel circuit where C_x and G_x are the measured capacitance and conductance under this configuration. To calculate the values of C_m and G_m, we have to correct the measured capacitance and conductance for G_s, C_p, and G_l using the following equations.

$$C_m = \frac{G_s^2(C_x - C_p)}{(G_s - G_x)^2 + \omega^2(C_x - C_p)^2} \tag{7}$$

$$G_m = \frac{G_s\{G_x(G_s - G_x) - \omega^2(C_x - C_p)^2\}}{(G_s - G_x)^2 + \omega^2(C_x - C_p)^2} - G_l\,. \tag{8}$$

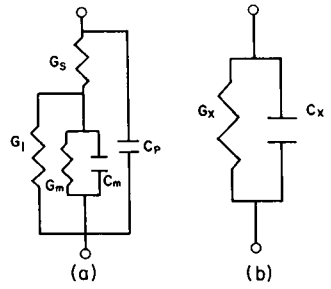

FIGURE 5 Electrical equivalent circuits for (*a*) whole-cell configuration and (*b*) the equivalent *G-C* parallel circuit where C_x and G_x are the measured whole-cell capacitance and conductance. In (*a*), G_s is series conductance, C_m and G_m are membrane capacitance and conductance, G_l is leakage conductance, and C_p is shunt electrode capacitance.

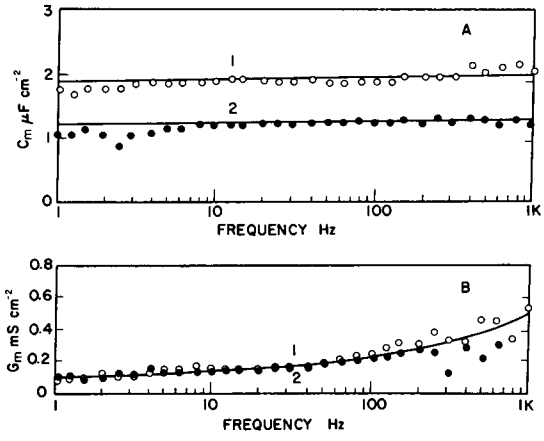

FIGURE 6 Frequency profile of the specific membrane capacitances and conductances of HeLa and myeloma cells. Curves 1 with open circles in both diagrams represent HeLa cells and curve 2 with filled circles represent myeloma cells.

As is obvious from Eq. 7, membrane capacitance C_m is not a function of G_l, whereas according to Eq. 8, the value of membrane conductance is strongly affected by the presence of leakage conductance G_l. In other words, whereas the presence of leakage conductance does not cause an error in the value of membrane capacitance C_m, membrane and leakage conductances are virtually inseparable, i.e., there is no unequivocal method to correct membrane conductance for G_l. An empirical method of the correction for leakage conductance G_l will be discussed in Appendix B.

It is shown in Appendix B that electrode capacitance C_p becomes virtually equal to the capacitance C_y obtained with the cell-attached or with the outside-out configurations (see Eq. B1). The value of G_s can be determined by the high frequency limiting conductance, likewise, in the cell-attached configuration (see Eq. B2). Therefore, we can easily solve Eqs. 7 and 8 by substituting the values of C_p and G_s. The total membrane capacitance and conductance thus obtained are shown by curve 4 in Fig. 4.

Fig. 6 shows the membrane capacitances and conductances of HeLa and myeloma cells per unit area. As clearly seen, neither HeLa nor myeloma membranes exhibit a frequency dependent capacitance between 1 Hz and 1 KHz. This behavior is somewhat different from the membrane capacitance of squid axon which is dependent on frequency (2). Mean values of the membrane capacitance were found to be 1.9 μFcm^{-2} for HeLa cells and 1.0 μFcm^{-2} for myeloma cells. These values are in good agreement with those obtained by the suspension technique as shown in Table 1. This agreement validates the results obtained with the micropipette technique. Unlike the suspension technique, this method is simple and straightforward in principle and provides unequivocal results on membrane capacitance and conductance, and furthermore, on their frequency characteristics. The latter two are the information which cannot be obtained by the suspension technique.

The membrane capacitance of HeLa cell, i.e., 1.9 μFcm^{-2} is considerably larger than the usual value of 1.0 μFcm^{-2}. This large value can be, however, attributed to the possible infolding of cell membrane. The actual membrane area, if infolding is taken into consideration, is much larger than the nominal area which is calculated from the apparent sphere assuming a smooth surface.

The membrane conductances of both HeLa and myeloma cells are of the order of 90–100 μScm^{-2}. These values are much smaller than that of excitable membranes such as nerve and muscle fibres, i.e., 0.5–1.0 $mScm^{-2}$ (16). Because the observed membrane conductance includes a small error due to leakage current of unknown magnitudes, the real membrane conductance would be even smaller than the one reported here. Because leakage conductance and membrane conductance are inseparable in the micropipette technique, the

TABLE 1 Membrane capacitances and conductances determined by the micropipette technique and suspension method

	No. exp.	Micropipette technique		Suspension method
		$C_m/\mu Fcm^{-2}$	$G_m/\mu Scm^{-2}$	$C_m/\mu Fcm^{-2}$
HeLa	8	1.85 ± 0.26	95 ± 12	1.99
Myeloma	6	1.03 ± 0.09	101 ± 25	0.87

The membrane capacitances and conductances determined by the micropipette technique are expressed as Mean ± S.E. The measurements were made at room temperature (25–28°C).

true membrane conductance will not be determined accurately.

The frequency independent membrane capacitance combined with a small membrane conductance indicate that the membrane of HeLa and myeloma cells, which are nonexcitable, are nearly a lossless capacitor. This observation appears to suggest that the membranes of HeLa and myeloma cells are a solid dielectric material in which membrane proteins are rigidly embedded in lipid matrices. The rotational freedom of membrane proteins which had been the primary interest of this study seems to be very limited in these membranes. These findings are not unexpected in view of the similar finding with erythrocyte membrane as reported previously (10).

APPENDIX A

Biological cells are represented by a single shell model, in which a conducting sphere (of complex relative permittivity ϵ^*_i) of a radius R is covered with a nonconducting shell (ϵ^*_m) of thickness d. Here, complex relative permittivity is defined as $\epsilon^* = \epsilon - jk/\omega\epsilon_v$, where ϵ is relative permittivity, k is conductivity, ω is angular frequency, ϵ_v is the permittivity of free space, and $j = \sqrt{-1}$. The equivalent homogeneous complex relative permittivity ϵ^*_c of a shelled sphere is given by

$$\epsilon^*_c = \epsilon^*_m \frac{2\epsilon^*_m + \epsilon^*_i - 2v(\epsilon^*_m - \epsilon^*_i)}{2\epsilon^*_m + \epsilon^*_i + v(\epsilon^*_m - \epsilon^*_i)}, \tag{A1}$$

where

$$V = \left(\frac{R}{R+d}\right)^3.$$

When the shelled spheres ϵ^*_c are suspended in a continuous medium (ϵ^*_a) at volume fraction P, the complex relative permittivity (ϵ^*) of the suspension is represented by Hanai's mixture equation.

$$\frac{\epsilon^* - \epsilon^*_c}{\epsilon^*_a - \epsilon^*_c}\left(\frac{\epsilon^*_a}{\epsilon^*}\right)^{1/3} = 1 - P. \tag{A2}$$

The combination of Eqs. A1 and A2 is termed the H-A-K equation, which has proven to provide good approximation of the dielectric behavior of cell suspensions.

Starting with the H-A-K equation, we derive an approximate equation, which enables us to calculate the membrane capacitance (C_m) using the measured dielectric parameters. Because biological cells generally satisfy the assumption that $k_m/k_i \ll 1$ and $d/R \ll 1$, the approximate equations of the limiting permittivity and conductivity of the shelled sphere at low frequencies (ϵ_{cl} and k_{cl}) are derived from Eq. A1 (for detailed derivation, see reference 13).

$$\epsilon_{cl} \simeq \epsilon_m \frac{(1+2v)}{(1-v)} \simeq \epsilon_m \frac{R}{d} = C_m \frac{R}{\epsilon_v} \tag{A3}$$

$$k_{cl} \simeq k_m \frac{(1+2v)}{(1-v)} \simeq k_m \frac{R}{d} = G_m \cdot R, \tag{A4}$$

where the membrane capacitance and conductances are defined by $C_m = \epsilon_m\epsilon_v/d$ and $G_m = k_m/d$, respectively.

In general, k_{cl} is much lower than the conductivity of the suspending medium (k_a) and the limiting conductivity of the suspension at low frequencies (k_l), so that the following approximate equations are derived from Eq. A2.

$$\frac{2\epsilon_l - 3\epsilon_{cl}}{2\epsilon_a - 3\epsilon_{cl}} \simeq \frac{k_l}{k_a} \tag{A5}$$

$$\frac{k_l}{k_a} \simeq (1-P)^{3/2}. \tag{A6}$$

Combining Eqs. A3 and A5, we obtain an approximate equation in which membrane capacitance (C_m) is a function of the measured parameters (ϵ_l, k_l, k_a, and R).

$$C_m \simeq \frac{2}{3} \cdot \frac{\epsilon_v}{R} \cdot \frac{\epsilon_l - \epsilon_a(k_l/k_a)}{1 - k_l/k_a}. \tag{A7}$$

If $\epsilon_l \gg \epsilon_a$, Eq. A7 will be further simplified.

$$C_m \simeq \frac{2}{3} \cdot \frac{\epsilon_v}{R} \cdot \frac{\epsilon_l}{1 - k_l/k_a}. \tag{A8}$$

APPENDIX B

One of the difficulties of the micropipette measurement of the whole cell admittance is the correction of the shunt capacitance of micropipette tip and leakage conductance. Namely, the shunt capacitance of an open micropipette is smaller than the one with its tip sealed with membrane (closed micropipette). Therefore, the use of the open tip capacitance entails an inadequate corrections for the shunt electrode capacitance. We substituted the capacitance obtained with the cell-attached or outside-out configurations for the shunt capacitance correction. This procedure is justified in the following.

The cell-attached configuration can be faithfully represented by an equivalent circuit shown in Fig. 7 *a*. The membrane of a cell is divided into two areas by the edge of the micropipette mouth. The capacitance and conductance of the patch inside the mouth are denoted by C_a and G_a and C_m and G_m for the area outside the tip. The area of the patch is negligibly small and, therefore, C_m and G_m can be ignored so that the

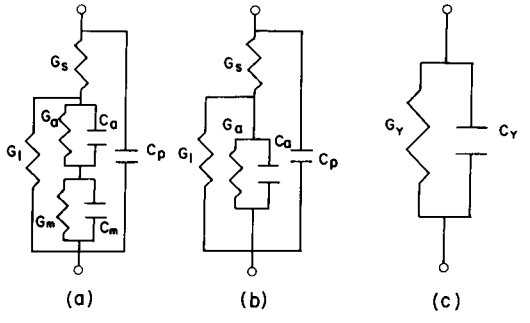

FIGURE 7 Electrical equivalent circuits of (*a*) cell-attached and (*b*) outside-out patch recording configurations. Model (*c*) is the equivalent parallel circuit of model (*b*) where C_y and G_y are the measured capacitance and conductance with this configuration. C_y and G_y should be differentiated from C_x and G_x.

circuit A reduces to B, i.e., the outside-out configuration. The model B reduces to a circuit C where C_y and G_y are represented by

$$C_y = \frac{C_a G_s (G_s - G_l - G_a)}{(G_s + G_l + G_a)^2 + \omega^2 C_a^2} + C_p \qquad \text{(B1)}$$

$$G_y = \frac{G_s\{G_s(G_l + G_a) + \omega^2 C_a^2\}}{(G_s + G_l + G_a)^2 + \omega^2 C_a^2}. \qquad \text{(B2)}$$

Our measurements indicate the following assumptions to hold: $G_s \gg G_l$, $G_s \gg G_a$, and $C_p \gg C_a$. Moreover, $G_s^2 \gg \omega^2 C_a^2$ below 1 KHz. Hence, Eqs. B1 and B2 are simplified to

$$C_y \simeq C_p + C_a \simeq C_p \qquad \text{(B3)}$$

$$G_y (= G_p) \simeq G_l + G_a \simeq G_l. \qquad \text{(B4)}$$

Thus, the subtraction of C_y and G_y from the measured capacitance and conductance of the whole cell effectively corrects the measured capacitance and conductance for the shunt electrode capacitance and also for the leakage conductance, provided that we can ignore the contribution of extremely small patch conductance G_a.

Received for publication 3 August 1989 and in final form 15 February 1990.

REFERENCES

1. Takashima, S., K. Asami, and R. E. Yantorno. 1988. Determination of electrical admittances of biological cells. *J. Electrostatistics.* 21:225–244.
2. Takashima, S., and H. P. Schwan. 1974. Passive electric properties of squid axon membrane. *J. Membr. Biol.* 17:51–68.
3. Fishman, H. M., D. Poussart, L. E. Moore, and E. Siebenga. 1977. K conduction description from the low frequency impedance and admittance of squid axon. *J. Membr. Biol.* 32:255–290.
4. Fishman, H. M., D. Poussart, and L. E. Moore. 1979. Complex admittance of Na conduction in squid axon. *J. Membr. Biol.* 50:43–63.
5. Falk, G., and P. Fatt. 1964. Linear electrical properties of striated muscle fibers observed with intracellular electrodes. *Proc. Roy. Soc. Lond. B.* 160:69–123.
6. Valdiosera, R., C. Clausen, and R. S. Eisenberg. Measurement of the impedance of frog skeletal muscle fibers. *Biophys. J.* 14:295–315.
7. Takashima, S. 1985. Passive electrical properties and voltage dependent membrane capacitance of single skeletal muscle fibers. *Pflugers Arch. Eur. J. Physiol.* 403:197–204.
8. Hamil, O. P., A. Marty, E. Neher, B. Sakmann, and E. J. Sigworth. 1981. Improved patch-clamp techniques for high-resolution current recording from cells and cell-free membrane patches. *Pfluegers Arch. Eur. J. Physiol.* 391:85–100.
9. Sakmann, B., and E. Neher. 1983. Single Channel Recording. Plenum Press, New York.
10. Takashima, S., K. Asami, and Y. Takahashi. 1988. Frequency domain studies of impedance characteristics of biological cells using micropipette technique. *Biophys. J.* 54:995–1000.
11. Armstrong, C. M., and F. Bezanilla. 1974. Charge movement associated with the opening and closing of the activation gates of the Na channels. *J. Gen. Physiol.* 63:533–552.
12. Keynes, R. D. and E. Rojas. 1974. Kinetics and steady state properties of the charged system controlling sodium conductance in the squid giant axon. *J. Physiol. (Lond.).* 239:393–434.
13. Asami, K., Y. Takahashi, and S. Takashima. 1989. Dielectric properties of mouse lymphocytes and erythrocytes. *Biochim. Biophys. Acta.* 1010:49–55.
14. Hanai, T., K. Asami, and N. Koizumi. 1979. Dielectric theory of concentrated suspensions of shell-sphere in particular reference to the analysis of biological cell suspensions. Bulletin of the Institute for Chemical Research, Kyoto University. 57:297–305.
15. Hanai, T. 1968. Dielectrical properties of disperse systems. *In* Emulsion Science. P. Sherman, editor. Academic Press, London. 353–478.
16. Cole, K. S. 1968. Membrane, Ions, and Impulses. University of California Press, Berkeley.